The effect of pore water pressure on structural performance of CERN concrete-lined tunnel

Zhipeng Xiao[1, 2], John Andrew Osborne[2], Eliseo Perez-Duenas[2], Zili Li[1, *]
[1] Civil, Structural & Environmental Engineering, University College Cork, Cork, Ireland
[2] European Center for Nuclear Research, CERN, Geneva, Switzerland
Email : zhipeng.xiao@ucc.ie, John.Andrew.Osborne@cern.ch, Eliseo.Perez-Duenas@cern.ch, zili.li@ucc.ie

ABSTRACT: The European Centre for Nuclear research (CERN) operates the most powerful circular particle accelerator in a large-scale underground tunnel network of over 70 km. Even over four decades after construction, substantial cracks, water infiltration and structural deformation have still been developing with time based upon field observation and measurements. In particular, recent blockage of tunnel drainage system alters the hydraulic boundary condition and results in the development of pore-water pressure around the tunnel circumference, which in turn accelerates the tunnel deterioration and leakage. In this study, the development of pore water pressure and its effect on tunnel lining are investigated using 3D hydro-mechanical coupled finite element modelling. In the numerical simulation, particular emphasis is placed on the change of lining permeability and the drainage system with time. Results show that the pore water pressure on tunnel lining is significantly affected by the change of hydraulic condition, and consequently exacerbates the tunnel structural performance in the long term.

KEY WORDS: Ageing tunnel; Hydro-mechanical coupled analysis; Lining permeability; Pore water pressure; Lining performance.

1 INTRODUCTION

The European Centre for Nuclear research (CERN) located in Geneva at the Swiss-French border operates the most powerful circular particle accelerator in a large-scale underground tunnel network of over 70km. These underground facilities, which consist of deep underground rings, shafts and tunnels, were excavated in a weak sedimentary rock formation called the "Molasse" region. It's a type of highly heterogeneous rock mass mainly composed of sub-horizontal layers of sandstone and marl with distinctly different mechanical properties [1,2]. Due to the complexity of the ground conditions, even over four decades after construction, substantial cracks, water infiltration and structural deformation have still been developing with time based upon field observation and measurements. A number of significant tensile and compressive cracks were also detected recently on the tunnel lining [3], requiring then an insightful understanding of the lining deformation mechanism behind the observed continuous tunnel structural deterioration.

Gradual deterioration of both the drainage systems and lining structure has been widely observed in many ageing tunnels worldwide. The hydraulic deterioration could be caused by the accumulation of transported material and squeezing of the geotextile by the self weight of the tunnel, and consequently hinder seepage into the tunnel [4-5]. Generally, most tunnels act as drains. The reduction in drainage capacity as a result of hydraulic deterioration causes the development of pore-water pressure on the tunnel lining, which in turn accelerate the tunnel deterioration and even leakage.

Previous works investigated the effect of groundwater seepage on tunnel performance. Zhang et al. [6] studies the ground and tunnel settlements induced by partial leakage of the shield tunnel, and found that partial tunnel leakage caused a great pore pressure reduction and a large ground surface settlement. Li et al. [7] investigated the impact of lining permeability on the long-term tunnel behaviour of cross passage in stiff London clay, and concluded that the more permeable lining is, the greater tunnel squatting deformation would be. In their analyses, nevertheless, the lining permeability was assumed to be uniform along the tunnel circumference and remained unchanged in the long term. On the other hand, Shin et al. [4] revealed that hydraulic deterioration causes significant changes in pore water pressure and structural behaviour due to the deterioration of joints and/or grouts in segmented linings. In addition to the increase of permeability caused by leakage, the reduction in drainage capacity due to blockage of tunnel drainage system is common in double-lined tunnel. To assess the effect of hydraulic deterioration of the drainage system, Shin et al. [8] developed a double-lined structural model incorporating hydraulic behaviour to represent the linings and drainage system, and found that hydraulic deterioration hinders flow into the tunnel, causing asymmetric development of pore-water pressure and consequent detrimental effects to the secondary lining.

Di Murro [9] conducted a series of soil-fluid coupled 2D finite element analyses to investigate the effect of pore water pressure on tunnel lining by applying pressure on tunnel circumference. Kim et al. [10] proposed a theoretical model of the hydraulic deterioration of tunnel geotextile filter to consider the mechanical and hydraulic behaviour of blinding, clogging and squeezing. However, the long-term hydraulic behaviour of ageing tunnel considering the degradation of drainage system has not been comprehensively investigated.

In this study, the long-term behaviour of a horseshoe shaped tunnel in the molasse rock mass called TT10 tunnel at CERN are investigated using 3D hydro-mechanical coupled finite element modelling. In the numerical simulation, particular emphasis is placed on the clogging phenomenon of drainage system with time represented by reducing the permeability of lining, to investigate the development of pore water pressure and its effect on tunnel lining.

2 CASE STUDY OF CERN TUNNEL

2.1 CERN TT10 tunnel

TT10 tunnel is an inclined transfer tunnel connecting the beam accelerator of the Proton Synchrotron (PS) tunnel to the Super Synchrotron Protons (SPS) ring. Unlike the main ring tunnels with a circular cross section, which were excavated by a full-face tunnel boring machine, TT10 tunnel was constructed in the 1970s in a horseshoe shape using an alpine boring machine called a road header.

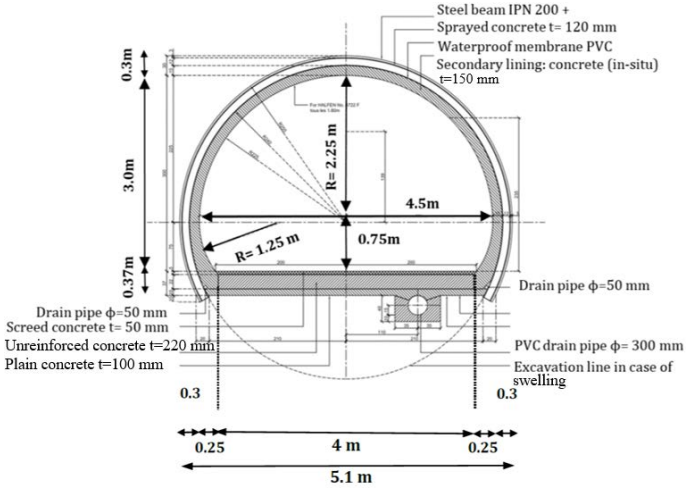

Figure 1. TT10 tunnel cross-section.

Figure 1 shows the cross section and support of TT10 tunnel. The tunnel has a diameter of 4.5 m at the intrados and 5.1 m at the extrados with a circular arc in the top roof and a flat bottom. The tunnel lining with a total thickness of 300 mm is composed of: the primary lining layer of sprayed concrete of 120 mm in thickness; a cast in-situ concrete layer of 150 mm thickness. In the floor section, a drainage system consists of two small drainage pipes at both sides of tunnel invert and a main drainage pipe below tunnel floor.

The TT10 tunnel excavation started in December 1972 and completed in the early of 1973. After construction, the tunnel acted as a flow channel as the surrounding groundwater seeps in through the water drainage pipes. However, after decades of tunnel operation, the drainage system deteriorates with decreasing permeability caused by the damage of drainage pipes and calcite deposits on tunnel drainage paths, distinctly altering new hydraulic boundaries condition around the tunnel. For example, in 2008, an early sign of groundwater ingress with calcite deposits was detected, and a camera inspection revealed the damage of drainage pipes and calcite deposition in drainage pipes.

2.2 Geological site

TT10 tunnel is entirely located in the molasse rock mass, characterised by sub horizontal bedded sequences of sandstones and marl layers [9]. The molasse region is overlain by Quaternary Moraine layers, glacial deposits which consist of gravels and sands with variable amounts of silt and clay [2].

A series of site investigation and laboratory testing were carried out in the area surrounding TT10 tunnel for the construction of CERN underground facilities. Furthermore, a number of geological face loggings with interval of 15 m along the tunnel chainage were traced during the TT10 tunnel excavation.

Based on the data interpretation in [9] and [11], and face-logs of TT10, the following main layers were identified within the molasse: medium-strong sandstones, Sandy marl, Weak marl and Very weak marl or “Lumpy” marl. The mechanical parameters of these rock/soil layers are listed in Table 1.

Table 1. Mechanical properties for the molasse and the moraine region.

Variable	Very weak marl	Weak marl	Sandy marl	medium-strong sandstones	Moraine	Concrete
Saturated density γ_{sat} [kN/m^3]	24	24	24	24	22.5	/
Earth pressure coefficient at rest k_0	1.2	1.5	1.5	1.5	1.5	/
Young’s modulus E[MPa]	270	555	1578	2754	50	20000
Poisson’s ratio υ	0.2	0.2	0.2	0.2	0.3	0.25
Effective cohesion c' [MPa]	0	3	11	15	0.1	/
Friction angle φ' [°]	25	-	-	-	31	/
Dilatancy ψ [°]	0	2	2	2	2	/
Permeability k [m/s]	1e-10	1e-9	1e-9	1e-8	1e-7	

3 FINITE ELEMENT MODELLING

3.1 Model geometry and boundary conditions

To investigate the long-term behaviour of the concrete-lined tunnel subject to drainage blockage, a series of 3D finite element numerical analyses were performed.

Considering symmetry, a 1/2 finite element model of TT10 tunnel was developed using ABAQUS 2019 [12] as shown in Figure 2. The model extended 120 m in length, 180 m in width and 70 m in height, which is set to minimise the undesired boundary effect. The depth of this tunnel section runs through from 23.9 m to 31.1 m below the ground surface. The lateral displacement boundaries were fixed in the horizontal direction but allowed to move vertically whereas the front side was assumed as a symmetrical plane. The movements at the bottom boundary were fixed, whereas the top was set to be free. The ground condition properties adopted in the analysis are showed in Table 1, while the initial pore water pressure was assumed hydrostatic with the water table at 4 m below the ground surface.

To reduce the computational time, a coarse mesh was employed at the far boundary with finer mesh around the tunnel section. The tunnel lining was modelled using shell elements, and shared the same nodes with surrounding soil elements at the tunnel boundary without modelling the interface. This was considered to be acceptable since the tunnel is unlikely to slip away from the surrounding ground during soil consolidation [7]. The whole 3D soil-fluid coupled model consists of 180107

elements and 86034 nodes. A Mohr-Coulomb constitutive model was adopted for all the soil layers, whilst a linear elastic model was assigned to lining.

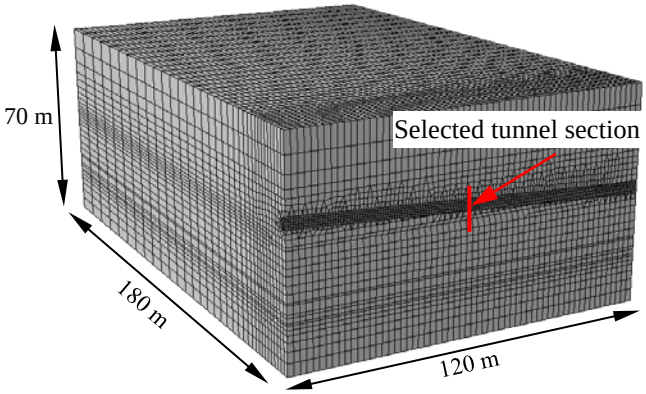

Figure 2. Finite element model of TT10 tunnel.

3.2 *Tunnel construction and long-term consolidation*

During tunnel excavation, the initial support of a thin layer of sprayed shotcrete was installed immediately after the excavation, then secondary lining support was installed thereafter. For brevity, the following construction stages were assumed in the FE modelling and summarised in Table 2. To simplify the step by step construction process, it was assumed the initial nodal loads around the tunnel boundary was reduced to a certain percentage (e.g. 50%) after the elements of excavated soil were removed and the lining 'shell' elements were then attached to the tunnel boundary.

Table 2. Construction stage assumed in the analysis.

Construction Stages	Description
1	Geostatic equilibrium
2	Remove the soil inside the tunnel and reduce the initial stress around the tunnel boundary to be 50%
3	Activate the linings element and further reduce the initial stress around the tunnel boundary to be 0%
4	Long-term ground consolidation
5	Swelling stage due to drainage blockage with decreasing lining permeability

3.3 *Numerical consideration of the deterioration of drainage system*

To investigate the effect of tunnel deterioration, two consideration were assumed: (1) the blockage of tunnel drainage system caused by fine particle accumulation; (2) the reduction of the lining stiffness due to the long-term structural deterioration as evidenced by cracks and concrete spalling. The clogging of drainage pipes was considered by reducing the permeability of the lining. Here, the extreme case of impermeable lining for the hydraulic boundary condition with the lining permeability of 1e-14 m/s was considered. Therefore, a swelling stage was also simulated by reducing the permeability and stiffness of the lining after the long-term soil consolidation stage.

4 RESULTS AND DISCUSSION

4.1 *Pore pressure distribution and tunnel deformation*

When the tunnel lining is fully permeable, the pore water will dissipate towards the tunnel leading to the pore pressure reduction around the tunnel. The dissipation of excess pore pressure with time leads earth pressure redistribution around the tunnel and consequently long-term tunnel deformation. In the long-term, the pore pressure around the tunnel will reduce to be zero until a new steady-state equilibrium condition is reached (Figure 3). In the event of drainage blockage due to hydraulic deterioration, the pore pressure would start to build up around the tunnel lining and in turn leads to further tunnel deformation.

In this study, a tunnel cross section with a depth of 27.5 m was selected for specific discussion, as marked in Figure 2, where geodetic surveying data of tunnel convergence has been gained. Figure 4 shows the change of pore pressure with time at four different positions around tunnel circumference during the swelling stage, where the start day 0 means the start of Stage 5. It can be observed that the pore pressure around the tunnel lining rapidly increases with time after the clogging of the drainage system. The pore pressure will build up to the initial hydrostatic pore water pressure after approximate 400 days.

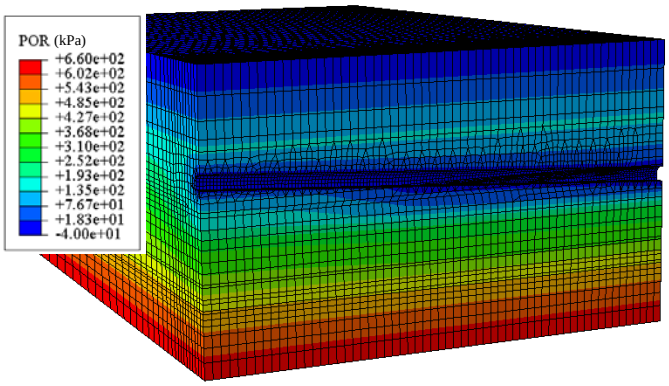

Figure 3. Distribution of pore water pressure at the end of consolidation stage.

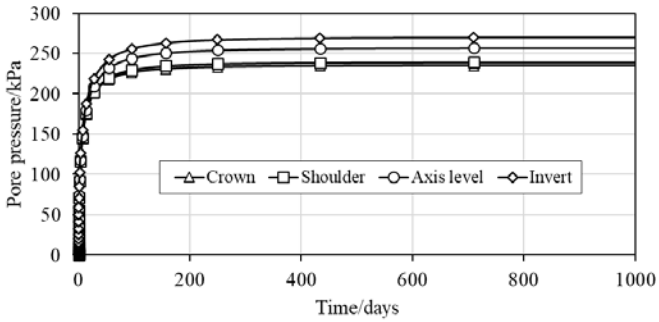

Figure 4. Change of pore pressure with time during the swelling stage.

In the interest of tunnel serviceability, continuous development of tunnel deformation with time may potentially affect the alignment and the integrity of the particle accelerator beamline at CERN. Figure 5 shows the horizontal and vertical displacements and the tunnel diameter change with time at the selected section. During the swelling stage, an increasing vertical displacement with the similar magnitude occurs at all

the 4 tunnel positions (e.g., tunnel crown, shoulder, invert), due to the uplift of tunnel by the increasing pore water pressure. Similar trend of horizontal displacements was also observed but with different magnitude for different positions. Here, both tunnel shoulder and axis level converge to tunnel, whereas the tunnel invert has the opposite behaviour. The changes in tunnel diameter shown in Figure 5(c) show that the tunnel lining is experiencing a decrease in the horizontal diameter with negligible vertical diameter change.

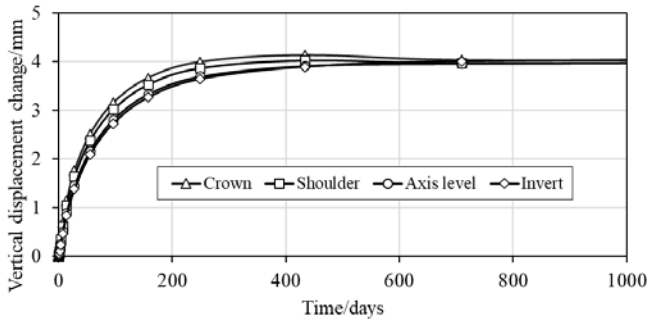

(a)

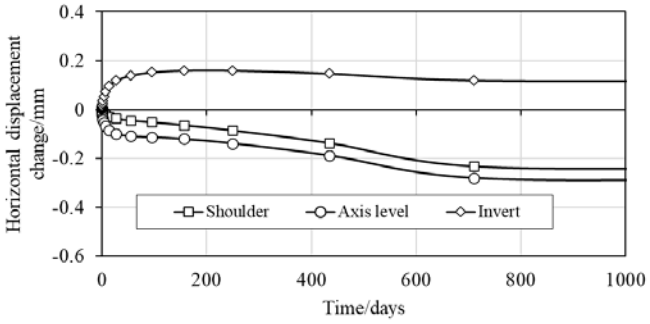

(b)

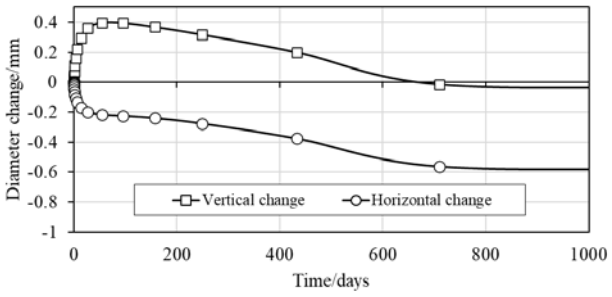

(c)

Figure 5. Tunnel deformation during swelling stage: (a) vertical displacement; (b) horizontal displacement; (c) change in tunnel diameter.

The computed deformation of tunnel lining was also confirmed by geodetic field measurements over the past 5 years, as given in Figure 6. The field data shows a decrease in the horizontal distance of the points at tunnel shoulder (distance between 3-6 in the figure), axis level (2-7) and invert (1-8), whilst the vertical distance (1-3 and 6-8) remains almost unchanged. Nevertheless, the computed tunnel deformation is only about half of the field measurement at the point of tunnel axis level. In particular, the measured horizontal distance (i.e. tunnel convergence) decreases linearly with time with no sign of stabilization.

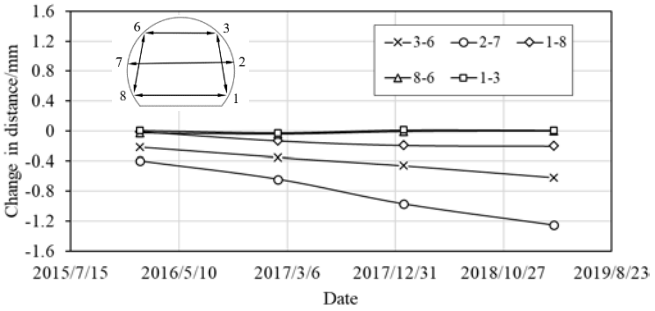

Figure 6. Field measurements: change in distances with time.

4.2 *Effect of permeability anisotropy*

The permeability anisotropy of soils is a key parameter because flow can occur much faster in one direction than another. Many factors, mostly related to macro and micro structure, are thought to control and cause permeability anisotropy. The permeability anisotropy has been noted in various rocks/soils [13-14]. To obtain the impact of permeability anisotropy on tunnel response, the vertical permeability k_v is kept unchanged and the ratio of horizontal permeability to vertical permeability (k_h/k_v) increased from 1(i.e., isotropic permeability) to 2, 5 and 10, respectively in the simulation. Numerical simulation results show that the final pore pressure acting on the lining was scarcely affected by the permeability ratios (Figure 7).

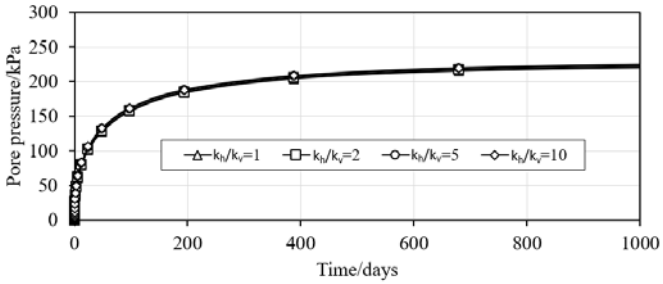

Figure 7. Change of pore pressure of tunnel crown during the swelling stage under various anisotropic permeability ratios.

Although negligible difference in pore pressure, significant changes in the horizontal displacement occurred in tunnel lining, as shown in Figure 8, when considering the permeability anisotropy. The final maximum horizontal displacement at point of tunnel axis level increases when the soil permeability ratios increase. For example, the maximum horizontal displacement is 0.29 mm, 0.37 mm, 0.47mm and 0.55 mm when the permeability ratio k_h/k_v is 1, 2, 5 and 10, respectively. And for the vertical displacement, the results presented in Figure 8 (a) show a small increase with the permeability ratios increase.

It should be noted that, in this study, the change of lining permeability was assumed to be applied instantaneously at the beginning of the swelling stage. However, the time-dependent change of lining permeability can simulate the tunnel deterioration more realistically as the clogging of tunnel drainage pipes is gradually occurred. Future investigations will consider the gradual lining permeability change to improve the understanding of hydraulic deterioration on the tunnel lining response.

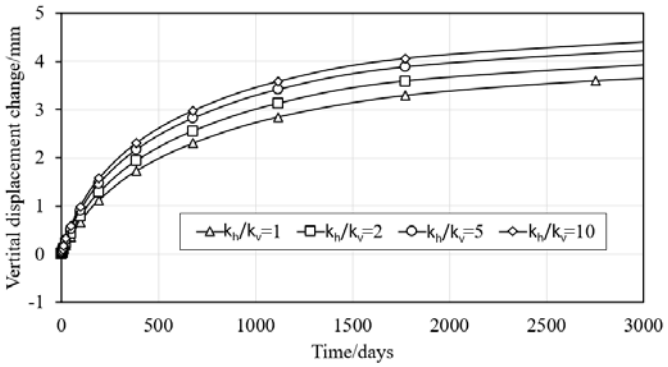

(a)

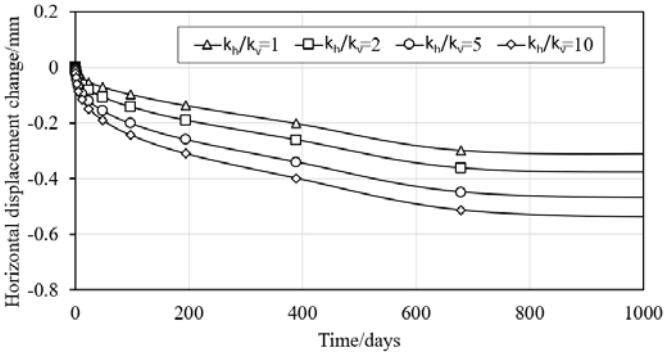

(b)

Figure 8. Displacement at point of tunnel axis level with various anisotropic permeability ratios during the swelling stage: (a) Vertical direction; (b) Horizontal direction.

5 CONCLUSION

This study conducted a series of 3D finite element numerical analysis to investigate the long-term behaviour of a horseshoe shaped CERN tunnel.

Finite element simulation, which takes into account the clogging phenomenon of drainage system, were performed to understand and predict the development of pore water pressure around tunnel and its potential effect on tunnel lining. In the FE model, the clogging of drainage system was simulated by reducing the permeability of lining. The significance of the hydraulic boundary has been identified. The results show that the blockage of drainage system caused a great pore water pressure increase around the tunnel circumference. Moreover, a decrease of tunnel diameter in horizontal direction was revealed by both the modelling and the field measurements. It also has been highlighted that ground permeability anisotropy has a strong impact on the lining deformation. The higher the ground permeability anisotropy ratio k_h/k_v is, the greater tunnel horizontal displacement develops.

Further analyses will investigate the time-dependent change of lining permeability due to the deterioration of drainage system and also compare the computed results against field measurements.

ACKNOWLEDGMENTS

The first author was supported by the funding from the European Union's Horizon 2020 research and innovation programme under the Marie Skłodowska-Curie grant agreement No 713279. This support is gratefully acknowledged.

REFERENCES

[1] Lombardi, G. (1979), 'Rock mechanics at the CERN proton-antiproton facilities', *In: International Society for Rock Mechanics, 4th ISRM International Congress on Rock Mechanics*, Balkema, Montreux, 433–436.

[2] Di Murro, V., Li, Z., Soga, K., and Scibile, L. (2018), 'Long-Term Behavior of CERN Tunnel in the Molasse Region', *GeoShanghai International Conference*, Singapore: Springer, 671-8.

[3] Di Murro, V., Pelecanos, L., Soga, K., Kechavarzi, C., and Scibile, L. (2016), 'Distributed fibre optic long-term monitoring of concrete-lined tunnel section TT10 at CERN', *Proceedings of the International Conference on Smart Infrastructure and Construction*, ICE Publishing, London, 27–32.

[4] Shin, J. H., Kim, S. H, and Shin, Y. S. (2012), 'Long-term mechanical and hydraulic interaction and leakage evaluation of segmented tunnels', *Soils and Foundations*, 52(1): 38-48.

[5] Shin, J. H., Potts, D. M., and Zdravkovic, L. (2005), 'The effect of pore-water pressure on NATM tunnel linings in decomposed granite soil', *Canadian Geotechnical Journal*, 42(6):1585-99.

[6] Zhang, D. M., Ma, L. X., Zhang, J., Hicher, P. Y. and Juang, C. H. (2015), 'Ground and tunnel responses induced by partial leakage in saturated clay with anisotropic permeability', *Engineering Geology*, 189, 104-115.

[7] Li, Z., Soga, K. and Wright, P. (2015), 'Long-term performance of cast-iron tunnel cross passage in London Clay', *Tunnelling and Underground Space Technology*, 50, 152-170.

[8] Shin, J. H., Lee, I. K., and Joo, E. J. (2014), 'Behavior of double lining due to long-term hydraulic deterioration of drainage system', *Structural Engineering and Mechanics*, 52(6), 1257-71.

[9] Di Murro, V. (2019), *Long-Term Performance of a concrete-lined Tunnel at CERN*, PhD Thesis, University of Cambridge, UK.

[10] Kim, K. H., Park, N. H., Kim, H. J., and Shin, J. H. (2020), 'Modelling of hydraulic deterioration of geotextile filter in tunnel drainage system', *Geotextiles and Geomembranes*, 48(2), 210-9.

[11] Fern, E.J., Di Murro, V., Soga, K., Li, Z., Scibile, L., and Osborne, J.A. (2018), 'Geotechnical Characterisation of a Weak Sedimentary Rock Mass at CERN, Geneva', *Tunnelling and Underground Space Technology*, 77, 249–60.

[12] Dassault Systemes, ABAQUS User's Manual, Version 2019, SIMULIA.

[13] Little, J. A., Wood, D. M., Paul, M. A., and Bouazaa, A., (1992), 'Some laboratory measurements of permeability of Bothkennar clay in relation to soil fabric', *Géotechnique*, 42(2):355-361.

[14] Sun, H., Vega, S., and Tao, G. (2018), 'Analysis of heterogeneity and permeability anisotropy in carbonate rock samples using digital rock physics', *Journal of Petroleum Science and Engineering*, 156, 419-429.